Miscibility and Crystallization of Poly(β-hydroxybutyrate) and Poly(*p*-vinylphenol) Blends

Peixiang Xing,* Lisong Dong, Yuxian An, and Zhiliu Feng

Polymer Physics Laboratory, Changchun Institute of Applied Chemistry, Chinese Academy of Sciences, Changchun 130022, Peoples Republic of China

M. Avella and E. Martuscelli

Istituto di Ricerche su Tecnologia dei Polimeri e Reologia del CNR, Via Toiano 6, 80072 Arco Felice, Naples, Italy

Received April 24, 1996; Revised Manuscript Received November 14, 1996[⊗]

ABSTRACT: The miscibility and crystallization behavior of poly(β-hydroxybutyrate) (PHB) and poly(*p*-vinylphenol) (PVPh) blends were studied by differential scanning calorimetry and optical microscopy (OM). The blends exhibit a single composition-dependent glass transition temperature, characteristic of miscible systems. A depression of the equilibrium melting temperature of PHB is observed. The interaction parameter values obtained from analysis of the melting point depression are of large negative values, which suggests that PHB and PVPh blends are thermodynamically miscible in the melt. Isothermal crystallization kinetics in the miscible blend system PHB/PVPh was examined by OM. The presence of the amorphous PVPh component results in a reduction in the rate of spherulite growth of PHB. The spherulite growth rate is analyzed using the Lauritzen−Hoffman model. The isothermally crystallized blends of PHB/PVPh were examined by wide-angle X-ray diffraction and small-angle X-ray scattering (SAXS). The long period obtained from SAXS increases with the increase in PVPh component, which implies that the amorphous PVPh is squeezed into the interlamallar region of PHB.

Poly(β-hydroxybutyrate) (PHB) is a polyester, which is biodegradable,[1] whether it is natural or synthesized. This polymer is a highly stereoregular biopolymer produced by many strains of bacteria as a storage medium.[2] PHB is highly crystalline and orthorhombic;[3] it has also been proved to be useful as a model material for the study of physical properties of polymers. For example, PHB has been found to be an excellent model material for the study of polymer nucleation because it contains no catalyst residues and has perfect tacticity, which is a result of biological origin.[4,5] PHB isolated from microorganisms is a biodegradable and biocompatible thermoplastic polymer. Consequently, microbial PHB has attracted much attention as an environmentally degradable resin to be used for a wide range of agricultural, marine, and medical applications.[6] However, practical use of PHB for these applications has been limited by its brittleness and narrow processing window. It is known that the growth of cracks within the large spherulites of PHB is the origin of its brittleness. Much work on blending it with other polymers to decrease the brittleness and melting point has been reported,[7−14] e.g., the miscibility of PHB and poly(ethylene oxide) (PEO) was studied.[11−13] The blends of PHB and PEO show a single glass transition temperature and a depression of both the equilibrium melting temperature of PHB and the growth rate of spherulites of PHB. The blends of PHB with poly(vinyl acetate) (PVAc)[14] were also found to be miscible. Furthermore, PHB, as an aliphatic polyester, has also been used to study the miscibility and crystallization behavior with other polymers,[15−24] such as PHB with poly(methyl methacrylate) (PMMA),[15,16] PHB with poly(epichlorohydrin) (PECH),[17,18] and especially PHB with synthesized atactic PHB (work done by Marchessault[19−21] and Doi[22] and their co-workers). Blends of PHB with the bacterial poly[(β-hydroxybutyrate)-*co*-(β-hydroxyvalerate)][23,24] containing less than 20 mol % of 3HV units are miscible in the melt. When PHB is isothermally crystallized from the melt, it forms regularly banded spherulites. Optical microscopy has been successfully used to measure the spherulitic growth rate of PHB due to its appropriate rate.

Generally, the phase behavior of polymer blends is governed by several factors: the molecular weights of the blend components, the blending process, and the specific polymer−polymer interaction (such as dipole−dipole, charge transfer, hydrogen bond, etc.). We chose poly(*p*-vinylphenol) (PVPh) with a proton donor and PHB with a proton acceptor as a blend pair and studied their miscibility and the crystallization behavior of PHB in the blends. The addition of an amorphous polymer into a semicrystalline polymer modifies both the melting (T_m) and the glass transition (T_g) temperatures of the crystalline polymer and consequently has an important effect on the kinetic parameters governing the crystallization process. Some work has been done on the blends of PHB/PVPh and atactic PHB/PVPh by Fernandez-Berridi and his co-workers.[25] However, their results only give the miscibility and T_gs of the two systems. The purpose of the present paper is to study the melt miscibility of PHB/PVPh by analysis of the glass transition temperature and the melting point depression as well as to examine the influence of the blend composition on the crystallization kinetics from the melt state.

Experimental Section

Materials and Specimen Preparation. The PVPh used in this study was purchased from Maruzen Corp. (M_n = 5200). The PHB was supplied by Aldrich, and its melting temperature is 172 °C. The molecular weight of PHB was measured by viscosity in chloroform and yielded M_n(PHB) = 2.93 × 10^5. These polymers were not purified when they were used.

Solution blending was used with a mixed solvent of tetrahydrofuran and chloroform (50/50 wt). Specimens were prepared by casting the solution onto glass slides and then dried under vacuum at 70 °C for 48 h, while those for wide-

[⊗] Abstract published in *Advance ACS Abstracts,* February 1, 1997.

S0024-9297(96)00615-8 CCC: $14.00

angle X-ray diffraction (WAXD) and small-angle X-ray scattering (SAXS) experiments were compression molded and isothermally crystallized at 90 °C for 24 h.

Experimental Conditions. A Perkin-Elmer DSC-2C differential scanning calorimeter was employed to study the glass transition temperature (T_g) and melting and crystallization behavior of PHB, PVPh, and their blends (PHB/PVPh). For glass transition temperatures (T_g) the samples were heated from 243 K to 463 K (first scan) with a heating rate of 10 K/min and then maintained at 463 K for 2 min before rapidly quenching to 243 K. The samples were then reheated to 463 K (second scan). The value of the midpoint of the transition was taken as the T_g.

For observing the melting temperature (T_m') as a function of the crystallization temperature (T_c), the samples were melted at 463 K for 2 min, quenched to the desired T_c, then isothermally crystallized until complete crystallization, and finally heated at a rate of 10 K/min in DSC. The melting peak temperature was taken as the melting point (T_m').

The radial growth rate of PHB spherulites at a given T_c was obtained by photographing from time to time during the isothermal crystallization process under an optical microscope. The radius growth rate ($G = dr/dt$) was calculated from the slope of the lines connecting the radius r and its time on a r vs t plot. The specimen on the hot stage was kept at 463 K for 2 min and then transferred as quickly as possible onto another hot stage at a prefixed T_c.

WAXD experiments were performed with a Philips PW1700 X-ray diffractometer using Cu Kα X-rays with a voltage of 30 kV and a current of 20 mA. SAXS measurements were also performed using the compact Kratky system connected with the Philips PW1700 diffractometer. The incident beam slit was 80 μm, and the receiving slit was 200 μm.

Results and Discussion

Glass Transition Temperature. Thermal characterization of polymer blends is a well-known method to determine the miscibility of polymer blends. Miscibility between any two polymers in the amorphous state is detected by the presence of a single glass transition temperature (T_g) intermediate between those of the two component polymers. Moreover, the T_g of a blend has an important effect on the mobility of the blend and hence on the rate of crystallization at a specified crystallization temperature. So it is important to establish the T_g behavior of PHB/PVPh blends. All the binary blends of PHB with PVPh give miscible systems according to the single T_g criterion. Figure 1 shows the DSC curves of the binary blends, from which it is seen that there exists only one T_g for each blend within the whole composition range. The values of T_gs are listed in Table 1. Cold crystallization was found in pure PHB and the blends containing a PVPh content up to 30% in the heating scan of quenched samples. Pure PHB showed a T_g of 276.5 K, which is close to the values 277−282 K given in the literature.[11,17,20] The T_g value found for PVPh is close to that reported in the literature, about 428 K.[26]

The dependence of T_g on the composition of the miscible PHB/PVPh blends is illustrated in Figure 2. For polymer blends their T_g values can be predicted by several equations such as the Fox equation,[27] Gordon−Taylor equation,[28] Couchman−Karasz equation,[29] Kwei equation,[30] etc. The Fox equation is shown as follows:

$$1/T_g = W_1/T_{g1} + W_2/T_{g2} \quad (1)$$

where W_1 and W_2 are the weight fractions of components 1 and 2, respectively (in the amorphous phase), and T_{g1} and T_{g2} are the respective T_gs of the pure components. Equation 1 (Fox equation) assumes random mixing

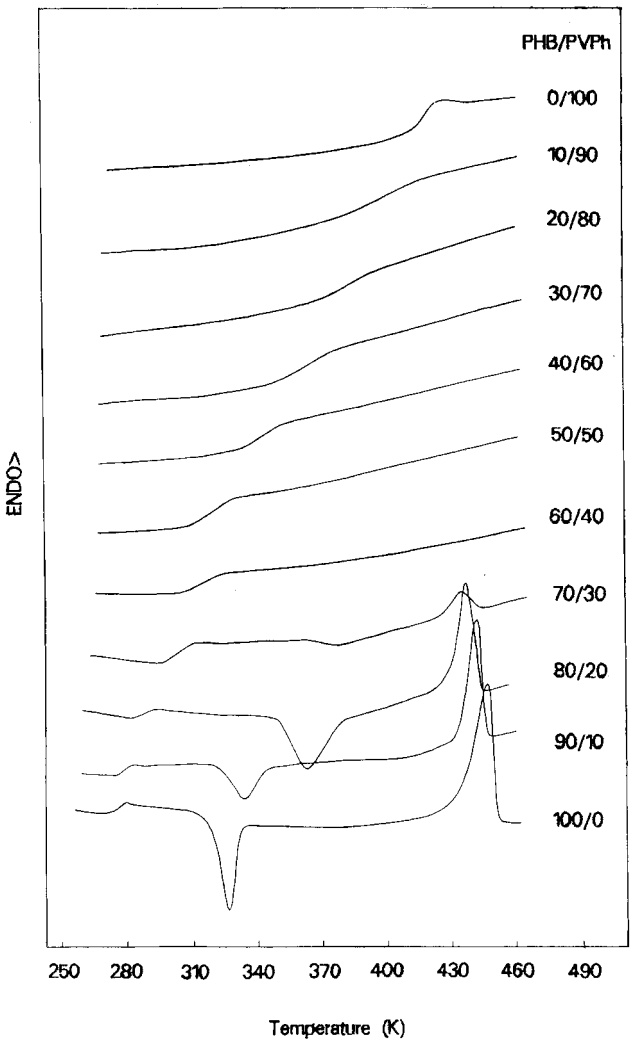

Figure 1. DSC curves recorded during heating at 10 K/min of quenched PHB, PVPh, and blends.

Table 1. Glass Transition Temperature(T_g) of Pure PHB, PVPh and PHB/PVPh Blends Obtained by DSC

PHB/PVPh	T_g (K)	PHB/PVPh	T_g (K)
100/0	276.5	40/60	343.7
90/10	285.4	30/70	362.1
80/20	295.1	20/80	386.0
70/30	305.7	10/90	397.3
60/40	317.2	0/100	417.0
50/50	328.3		

between the blend components, equal values of the differences between specific heats of the liquid and the glassy states in the glass transition range of the two components (i.e., $\Delta Cp_1 = \Delta Cp_2$), and no volume expansion between the two components during mixing. The predicted curve by the Fox equation is shown in Figure 2 (curve a) using T_g(PHB) = 276.5 K and T_g(PVPh) = 417 K.

From the figure it is seen that only T_gs of several blends containing a high PVPh content fit the Fox equation and all other experimental T_gs lie below the predicted curve. In this case the heat capacity of the polymer components should be considered. So the Couchman−Karasz equation was chosen to predict the glass transition behavior of the PHB/PVPh blends:

$$\ln T_g = (w_1\Delta Cp_1 \ln T_{g1} + W_2\Delta Cp_2 \ln T_{g2})/(W_1\Delta Cp_1 + W_2\Delta Cp_2) \quad (2)$$

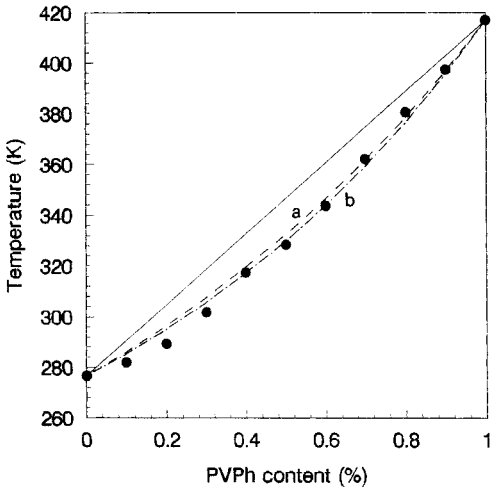

Figure 2. Glass transition temperature (T_g) versus composition of PHB/PVPh blends: (●) experimental points; curve a was calculated using the Fox equation; curve b was calculated using the Couchman−Karasz equation.

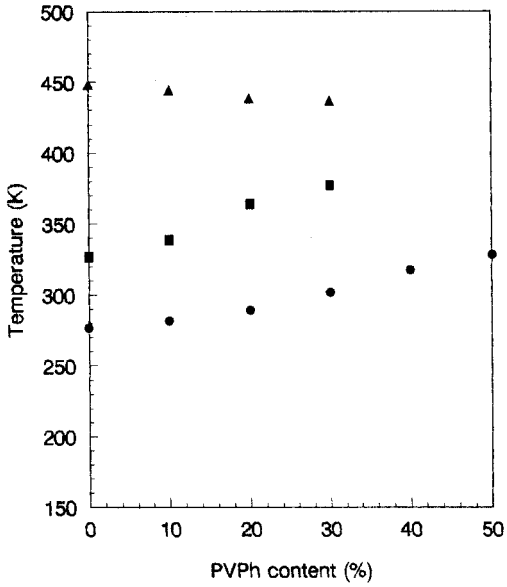

Figure 3. Experimental melting point (▲), cold crystallization peak temperature (■), and glass transition temperature (●) of PHB/PVPh quenched blends as a function of blend composition.

Where ΔCp_1 and ΔCp_2 are the respective heat capacities of the pure components. In this study the values of the capacities of PHB and PVPh were measured by DSC. ΔCp_1 is 0.626 J g^{-1} K^{-1} for PHB and ΔCp_2 is 0.472 J g^{-1} K^{-1} for PVPh. The value of the heat capacity of PVPh is close to the value reported by Cortazer.[31] As shown in Figure 2, the T_g values of the blends of high PHB content (up to 60%) are lower than those predicted by either the Fox or Couchman−Karasz equation (curve b). However, with the exception of these, the T_g of the blends versus composition curve fits the Couchman−Karasz equation better than the Fox equation.

Cold Crystallization and Heat of Fusion. The cold crystallization peak of the quenched blends (see Figure 1) moves toward higher temperatures with the increase in PVPh content. The increase in the cold crystallization peak temperature observed for the quenched blends with composition 90/10 to 70/30 (see Figure 3) can be explained by considering that the crystallization process takes place from a single homogeneous phase. The T_g of this phase increases with the PVPh content. Generally, the cold crystallization may take place at a high enough temperature above the T_g of the blends (as in Figure 3) where the crystallizable polymer chains possess enough segmental mobility to crystallize. In this case, the glass transition temperature of the amorphous polymer PVPh is of prime importance for the crystallization of the semicrystalline polymer PHB. When PVPh reaches 40%, cold crystallization (PHB(60)/PVPh(40) wt) could not take place due to the high T_g of this blend.

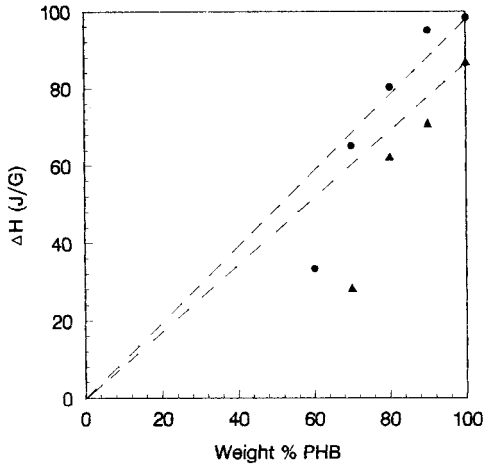

Figure 4. Heat of fusion of PHB/PVPh blends: (▲) quenched samples and (●) isothermally crystallized samples (at 90 °C).

With reference to the heats of fusion for the quenched samples, blends containing more than 10% PVPh move away from the line that represents the melting enthalpy of pure PHB and the melting enthalpy of PHB in the blend approaches zero at about 40% PVPh content. This means that the crystallization process could not be completed in this case. On the contrary, referring to the heats of fusion of the isothermally crystallized blends, as shown in Figure 4, blends with a PHB content higher than 60% give values that fall very close to the line which expresses the melting enthalpy of PHB in the pure state. Hence, it may be considered that in these blends PHB crystallizes to an extent similar to that in the pure state. Such behavior has also been observed for poly(vinylidene fluoride) (PVDF)/poly(methyl methacrylate) (PMMA).[32]

Equilibrium Melting Temperature and Melting Point Depression. Analysis of the melting behavior of crystalline polymer blends is an important way of assessing polymer−polymer miscibility. Thermodynamic considerations predict that the chemical potential of a polymer will be decreased by the addition of a miscible diluent. If the polymer is crystallizable, this decrease in chemical potential will result in a decreased equilibrium melting point. The extent of the melting point depression in such systems provides a measure of the interaction parameter which is described by Flory−Huggins theory.[32,33] The equilibrium melting temperature can be derived from the Hoffmann−Weeks equation[34] which is a very convenient method:

$$T_m' = T_c/\gamma + (1 - 1/\gamma)T_m^\circ \qquad (3)$$

T_m' is the observed melting point, T_c is the isothermal crystallization temperature, T_m° is the equilibrium melting point, and γ is the ratio of the initial to the final lamellar thickness. The Hoffman−Weeks equation predicts a linear relation between T_m' and T_c. The equilibrium melting point T_m° is obtained from the

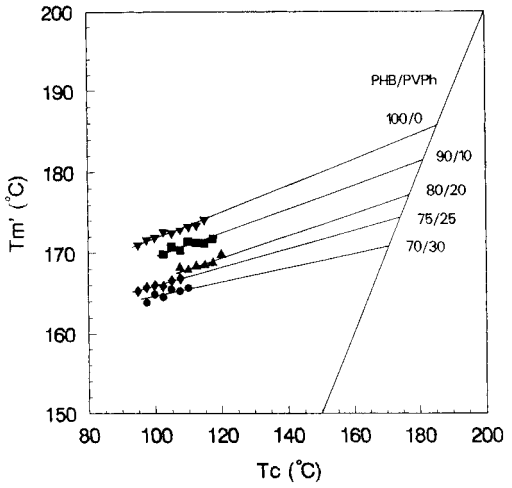

Figure 5. Hoffman–Weeks plots for PHB/PVPh blends employing data from DSC: (▼) 100/0, (■) 90/10, (▲) 80/20, (♦) 75/25, and (●) 70/30.

Table 2. Equilibrium Melting Temperature ($T_m°$) for Pure PHB and PHB/PVPh Blends

PHB/PVPh	$T_m°$ (°C)
100/0	186
90/10	182
80/20	177
75/25	174
70/30	171

intersection of the line with the line of the $T_m' = T_c$ equation, which implies the extrapolation to infinite thickness of lamella.

The change of the observed melting point, T_m' with T_c for pure PHB and for PHB crystallized from the blend was studied by DSC (Figure 5). Generally, the $T_m°$ obtained from eq 3 is affected by the experimental conditions such as crystallization temperature range, time of crystallization, and scanning rate. Under the conditions described in the Experimental Section, Figure 5 gives the best-fit T_m' *versus* T_c lines for PHB/PVPh blends. So the equilibrium melting point of the polymer blends of PHB/PVPh was obtained. The values of $T_m°$ for blends determined by this method are listed in Table 2. In this system we found that the equilibrium melting point of pure PHB is lower than that reported in the literature.[4,11,20] Perhaps it is due to the molecular weight difference. It is clearly seen that the equilibrium melting point shows a decrease with the increase in the amorphous component PVPh. The fact that the melting point depression is well observed in the PHB/PVPh blends means that the PHB/PVPh blends are miscible blends.

It is well known that miscibility in polymer–polymer blends is controlled by a thermodynamic process. As reported, several techniques have been used to determine χ_{12}. In this work, the melting temperature depression method is employed because one of the components is semicrystalline and the other component is amorphous. So we may get the Flory–Huggins interaction parameter χ_{12} using the Flory–Huggins equation:[32]

$$1/T_m°' - 1/T_m° = -(BV_{2u}/\Delta H_f V_{1u})[\ln \phi_2/m_2 + (1/m_2 - 1/m_1)\phi_1 + \chi_{12}\phi_1^2] \quad (4)$$

where $T_m°'$ and $T_m°$ are the equilibrium melting points of the blend and homopolymer, respectively, ΔH_f is the heat of fusion for the 100% crystallizable component,

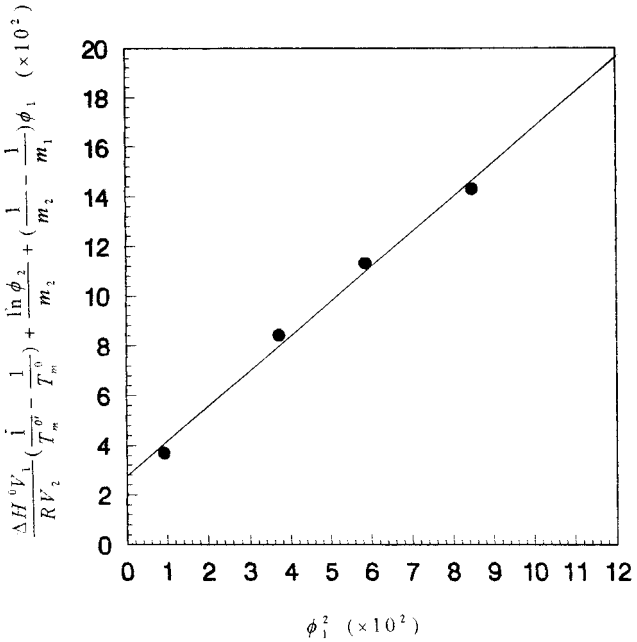

Figure 6. Application of the Flory–Huggins equation for PHB/PVPh blends.

V_{1u} and V_{2u} are the molar volumes of the repeat units of the noncrystallizable and crystallizable components, and m_1, ϕ_1 and m_2, ϕ_2 are the degrees of polymerization and the volume fractions of noncrystallizable polymers 1 and crystallizable polymer 2, respectively. Equation 4 may be applied to PHB/PVPh blends. By rearranging, eq 5 is obtained as follows:

$$-[\Delta H V_{1u}/R V_{2u}(1/T_m°' - 1/T_m°) + \ln \phi_2/m_2 + (1/m_2 - 1/m_1)\phi_1] = \chi_{12}\phi_1^2 \quad (5)$$

A plot of the left-hand side of eq 5 versus ϕ_1^2 should give a straight line passing through the origin if χ_{12} is assumed to be independent of composition. In order to calculate the left-hand side of eq 5, the parameter values used are as follows: V_1 (=100 cm^3)[35] is the repeat unit molar volume of PVPh, V_{2u} (=75 cm^3)[11] is the repeat molar volume of PHB, and ΔH_f (=3001 cal)[11] is the enthalpy of fusion for completely crystalline PHB. The line passing through the experimental points intercepts the axis at 0.028 and a slope of −1.4 (Figure 6). The fact that this line does not pass through the origin is usually attributed to a residual entropic effect which is neglected in the derivation of the equation. Such results were already reported by Paul et al.[36–38] In a PHB/PVPh blend system, we approximately treat the slope of the line in Figure 6 as the Flory–Huggins interaction parameter due to the very small positive intercept (0.028). The unusually large negative value of χ_{12} clearly indicates that PHB and PVPh are miscible in the melt due to the strong specific interactions (intermolecular hydrogen bonding) in the amorphous phase and on the periphery of the crystallites between PHB and PVPh. This kind of large negative interaction parameter has already been obtained using the Nishi–Wang equation[32] by Qin et al. for PEO/PVPh blends,[35] which is due to the strong intermolecular hydrogen bonding.

Crystallization Behavior. The spherulite growth rates of pure PHB and PHB/PVPh blends were determined by observation with a polarizing optical microscope. Thin films of PHB/PVPh blends isothermally

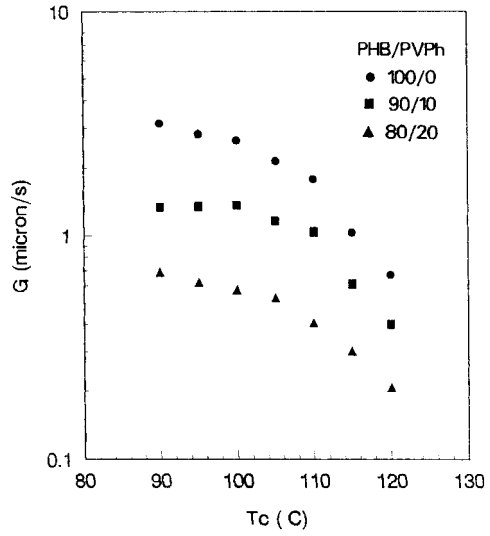

Figure 7. Dependence of the spherulite growth rate with the crystallization temperature for PHB/PVPh blends: (●) 100/0, (■) 90/10, and (▲) 80/20.

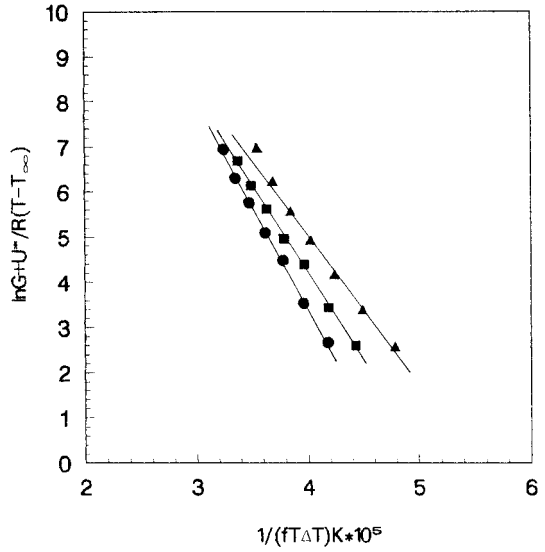

Figure 8. Kinetic analysis of crystallization rate constant data employing WLF transport constants and $T_m°$ values obtained by DSC for PHB/PVPh blends: (●) 100/0, (■) 90/10, and (▲) 80/20.

crystallized in the temperature range 363−393 K showed a spherulitic morphology for all compositions examined. The spherulite growth rate, G, was constant until impingement took place. The dependence of G on T_c is shown in Figure 7. As can be seen in Figure 7, for PHB/PVPh blends the rate of spherulite growth at a given T_c decreases with the increase in PVPh content. The presence of the amorphous and high-T_g PVPh in blends remarkably decreases the rate of PHB crystallization. Generally, there are three main factors that can be taken into account to explain the crystallization rate depression in miscible semicrystalline/amorphous polymer with high T_g, (a) a dilution effect which diminishes the formation of a critical nucleus on the front of the growing spherulite, (b) a decrease of segmental mobility of the semicrystalline polymer molecules due to the high T_g of the blends, and (c) a decrease in undercooling due to the melting point depression. Crystallization rate depression of a magnitude similar to the ones shown in Figure 8 has been reported for miscible blends of PVDF/PMMA.[32] In the PVDF/PMMA system the growth rate decrease was mainly attributed to the changes in fluidity of the melt caused by the higher T_g of the blends than the pure PVDF. Similarly, the same reason may be used to explain the growth rate depression in the PHB/PVPh system.

The Lauritzen−Hoffmann equation[39] was used to analyze the spherulite crystallization behavior of PHB/PVPh blends. The equation is shown below:

$$G = G_o \exp[-U^*/R(T - T_\infty)] \exp(-K_g/fT\Delta T) \quad (6)$$

where the pre-exponential factor G_o contains terms which are essentially temperature-independent. U^* is the activation energy for transportation of crystallizable segments to the crystallization front. T_∞ is the temperature below which such motion ceases, T is the crystallization temperature, $\Delta T = T_m - T$ is the degree of undercooling, and T_m is the equilibrium melting point. f is a factor which accounts for the variation in the enthalpy of fusion (Δh_f) with temperature and is given by $f = 2T/(T_m + T)$. K_g is the nucleation constant and can be expressed as:[39,40]

$$K_g = nb_o\sigma\sigma_e T_m/\Delta h_f K \quad (7)$$

where σ and σ_e are the lateral and end surface free energies, respectively, of the growing crystal, b_o is the molecular thickness, and K is the Boltzmann constant. The value of n depends on the regime of crystallization.

It is important to note that the parameter U^* and T_∞ (eq 6) were treated as variables in order to maximize the quality of the fit to eq (7). In many cases in the literature these parameters have simply been assigned the "universal" values[39] $U^* = 1500$ cal mol^{-1} and $T_\infty = T_g - 30$ K, as appropriate to many polymers, or the Williams−Landel−Ferry (WLF)[41] values $U^* = 4120$ cal mol^{-1} and $T_\infty = T_g - 51.6$ K.

It is often most convenient to rearrange eq 7 as follows:

$$\ln G + U^*/[R(T - T_\infty)] = \ln G_o - K_g/[T(\Delta T)f] \quad (8)$$

and to examine the growth rate data in the form of a plot of the left-hand side of eq 8 vs $1/[T(\Delta T)f]$, where the slope is $-K_g$. The K_g obtained with the above analysis from Figure 8 is 4.74×10^5 (K^2) for pure PHB, which is close to the results reported in the literature by Martuscelli.[14] Besides, some results have already been obtained for the pure PHB[20] and blends containing PHB.[20] It is found that the regime transition from regime II to regime III exists in the crystallization process of PHB and atactic PHB blends at about 120−140 °C. So in our analysis the regime is assigned to be regime III, and $n = 4$ was adopted. The derived K_gs can be used to calculate σ_e (and the work of chain folding (q)) for the PHB. We make use of the empirical relation:[42]

$$\sigma = \alpha(\Delta H_f)(a_o b_o)^{1/2} \quad (9)$$

with $\alpha = 0.25$ as appropriate for high-melting polyesters (e.g., poly(pivalolactone)[43] and poly(phenylene sulfide)[44]), and using literature values of $a_o = 6.6$ Å, $b_o = 5.8$ Å,[4] and $\Delta H_f = 1.85 \times 10^8$ J m^{-3} and eq 9 yield $\sigma = 29$ erg cm^{-2} and $\sigma_e = 42.74$ erg cm^{-2} (Table 3). The latter value agrees well with a previously reported value of 38 ± 6 erg cm^{-2} determined by measurements of lamellar thickness.[4] These values are different from the values (96 erg cm$^{-1/2}$) reported for PHB and poly(epichlorohydrin).[17] The reason pointed out by Marches-

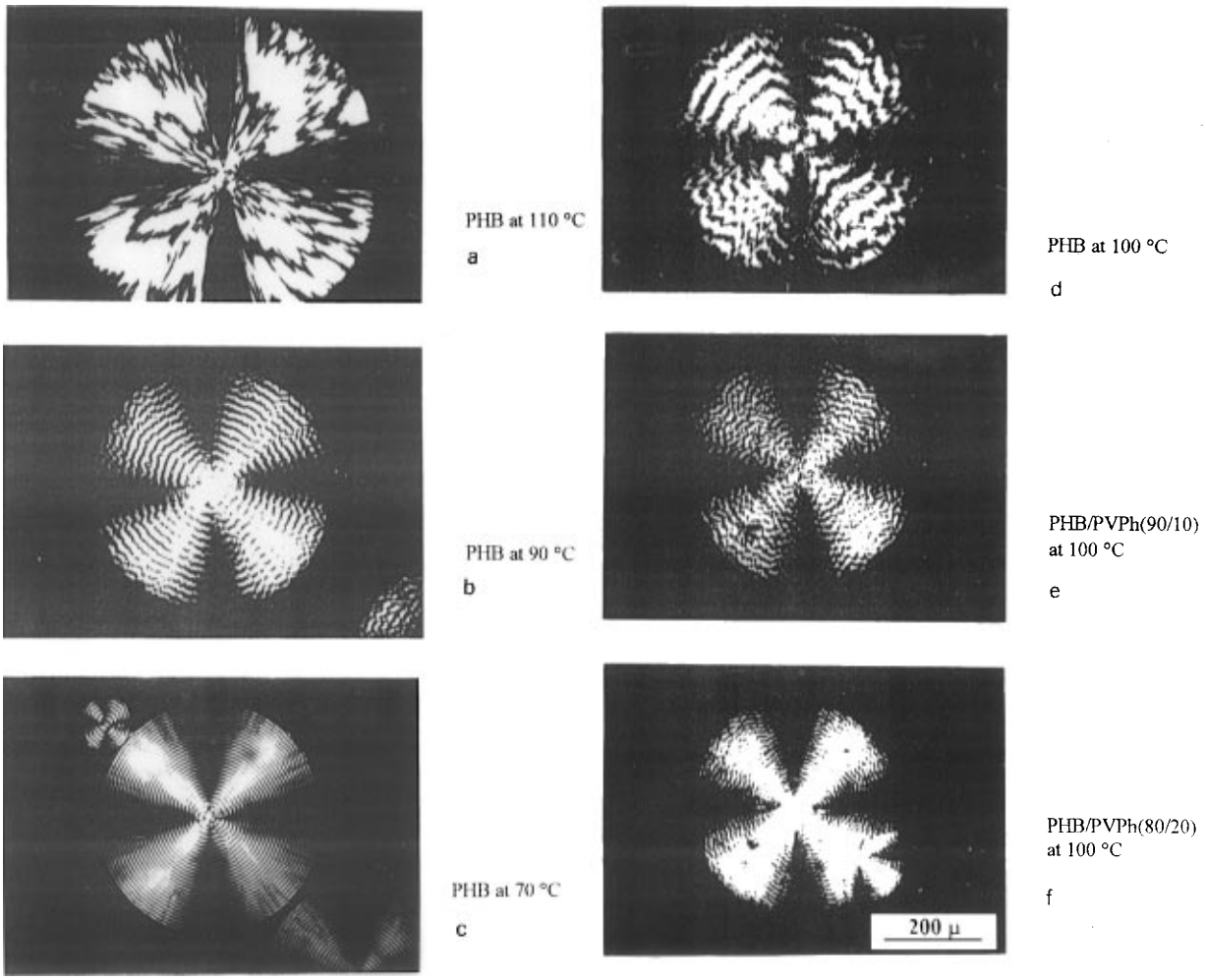

Figure 9. Optical micrographs (cross-polars) of isothermally crystallized pure PHB and PHB/PVPh blends: (a) PHB at 110 °C, (b) PHB at 90 °C, (c) PHB at 70 °C, (d) PHB at 100 °C, (e) PHB/PVPh (90/10) at 100 °C, and (f) PHB/PVPh (80/20) at 100 °C.

Table 3. Values of K_g and σ_e for Pure PHB and PHB/PVPh Blends

PHB/PVPh	Kg(III) (K^2)	σ_e (erg cm^{-2})
100/0	4.61×10^5	42.74
90/10	3.90×10^5	33.48
80/20	3.31×10^5	28.75

sault[21] is due to the value of α. K_g value decreases with the increasing of PVPh content. The σ_e values for blends are lower than that for pure PHB.

Morphology. Presented below are some results of our work on the crystalline structure of this miscible blend of PHB/PVPh with the aid of optical microscopy, WAXD, and SAXS techniques.

The spherulites exhibit a typical banded structure. The band spacing changes with isothermal crystallization temperature and PVPh content. For pure PHB the band spacing decreases with the decrease in isothermal crystallization temperature (Figure 9a−d). This kind of spherulite morphology for pure PHB was reported by Keller et al.[4] At constant crystallization temperature, the band spacing decreases with the increase in PVPh content (Figure 9d−f and Figure 10). Generally, the banded structure of spherulite as reported in the literature[45] is due to the existence of twisted lamellae resulting from stress build up during crystallization and probably occurring within disordered fold surfaces of polymer crystals. Li et al.[46] reported that PCL formed banded spherulites when it was blended with SAN and the band spacing decreased with the increase in SAN

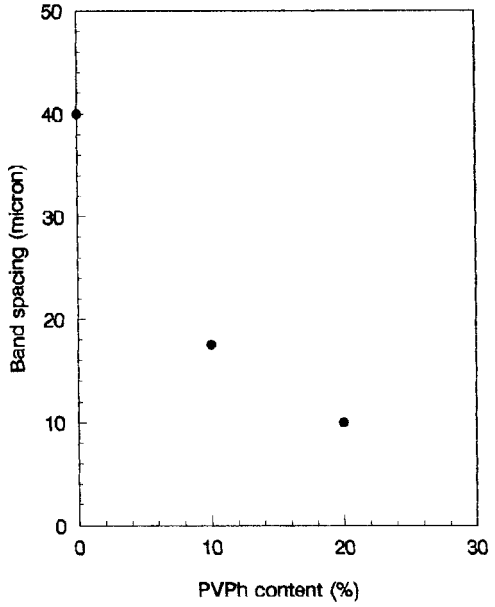

Figure 10. Band spacing in the isothermally crystallized pure PHB and PHB/PVPh blends.

component. Hence one possible explanation for this change of band spacing in the spherulites of PHB/PVPh blends is that the rejection of PVPh with high T_g from crystalline lamellae to an interlamellar amorphous region will give rise to stress on the lamellar sufaces and result in twisted lamellae during crystallization.[47]

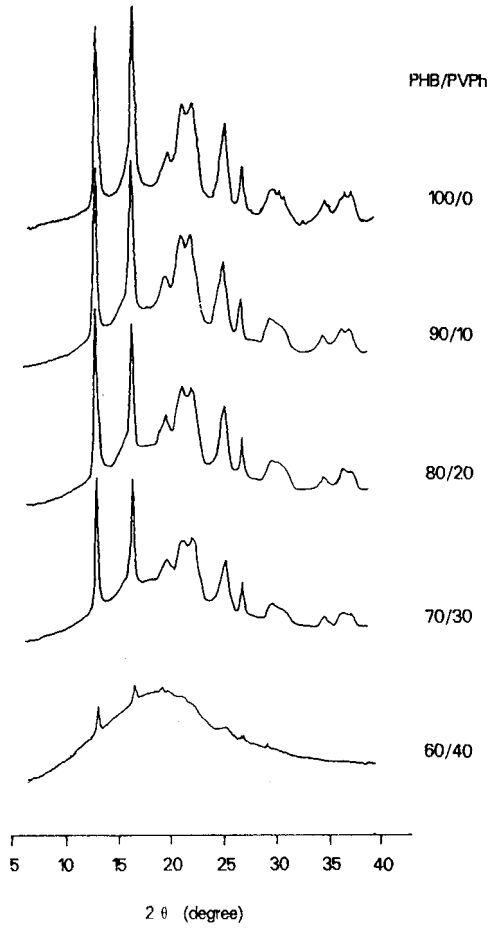

Figure 11. WAXD profiles of isothermally crystallized (at 90 °C) PHB/PVPh blends.

Therefore, the stress should be larger for higher PVPh content, and the twist period should be shorter.

Studies on the structure of the crystallized PHB in its blends were also carried out with WAXD and SAXS. The X-ray diffraction results are shown in Figure 11. Comparing the spectrum of the pure PHB with that of the blends, it is seen that the *d*-spacing values are constant for the (1 1 0), (0 0 2), and (0 2 0) crystallographic planes, which indicates that the PHB unit cell is not changed in the blends. Meanwhile the simulating results also show that the unit cell parameters are the same in both pure PHB and PHB in blends. The intensities of the crystalline peaks of pure PHB and PHB/PVPh (90/10) are almost the same, while the intensities of the crystalline peaks of PHB/PVPh (80/20, 70/30, and 60/40) decrease obviously, which implies that the addition of PVPh will hinder the crystallization of PHB in the blend, when the content of PVPh is higher than 10 wt %.

The desmeared SAXS profiles of the isothermally crystallized pure PHB and PHB/PVPh blends (Figure 12) show the presence of a maximum, which is associated with the long period between the centers of adjacent lamellae. It is clearly seen that the long period increases with the increase in PVPh content. This suggests that during crystallization of PHB from the one-phase melt, the amorphous PVPh is being rejected into the interlamallar region of PHB, where it forms a homogeneous mixture with the amorphous part of PHB molecules. It has been shown in the literature that the nature of the segregation process (interlamellar, interfibrillar, or interspherulitic) in a miscible blend of a

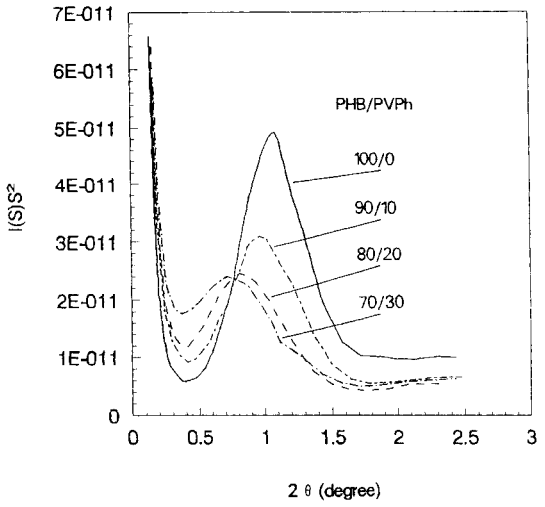

Figure 12. Desmeared SAXS profiles of isothermally crystallized (at 90 °C) PHB/PVPh blends: (a) 100/0, (b) 90/10, (c) 80/20, and (d) 70/30.

Table 4. Long Period Values (Å) for Isothermally Crystallized (at 90 °C) Pure PHB and PHB/PVPh Blends

PHB/PVPh	long period (A)
100/0	81.2
90/10	92.1
80/20	104.5
70/30	123.4

crystallizable polymer with an amorphous one depends on the type of the amorphous polymer. Some experimental evidences[48,49] are given that the glass transition temperature of the amorphous polymer is one of the main parameters controlling its segregation behavior in a miscible binary blend during isothermal crystallization of the crystallizable component. For example, Martuscelli et al.[18] reported that decreases in the long period and equilibrium melting point were found in PHB/PECH with increasing the PECH content. So the amorphous PECH exists in an interfibrillar region. The dissimilar segregation behavior between PHB/PVPh and PHB/PECH blends may be attributed to the difference in T_gs of the amorphous polymers (T_g of PVPh is 144 °C and T_g of PECH is −20 °C). The chain mobility of PECH molecules in its blend with PHB is much higher, and as a consequence, these molecules diffuse quickly away from the crystallization nucleus during the lamellar growth process of PHB.

Conclusions

A systematic study of the miscibility, crystallization, and morphology of PHB/PVPh blends has been performed. The single glass transition temperatures of the blends suggest that PHB and PVPh will form miscible blends in the whole composition range in melt. After quenching, the melting enthalpy of PHB in the blend is substantially lowered and approaches zero at about 40% PVPh content, which is due to the high glass transition temperature of the blend. The equilibrium melting point of PHB in the blends, which was obtained from DSC results using the Hoffman−Weeks equation, decreases with the increase in PVPh content. The large negative values of the interaction parameter determined from the equilibrium melting point depression support the miscibility and strong hydrogen-bonding interactions between the components. It is found that the rate of isothermal crystallization of PHB is strongly affected by blending it with PVPh. The rate of spherulite growth

decreases with the increase in PVPh content. The kinetics of crystallization of PHB were analyzed according to nucleation theory in the explored temperature range. The best fit of the data to the kinetic theory is obtained by employing WLF parameters and the equilibrium melting points obtained by DSC. Isothermally crystallized blends of PHB with PVPh were examined by WAXD and SAXS. The long period increases with the addition of amorphous PVPh, which is a strong indication for an interlamellar segregation.

Acknowledgment. The authors are grateful for financial support granted by The National Key Projects for Fundamental Research "Macromolecular Condensed State", The State Science and Technology Commission of China.

References and Notes

(1) Doi, Y. *Microbial Polyesters*; VCH: New York, 1990.
(2) Dawes, E. A. *Microbial Energetics*; Blackie: Glasgow, U.K., 1986.
(3) Yokouchi, M.; Chatani, Y.; Teranishi, K.; Tani, H. *Polymer* **1973**, *14*, 267.
(4) Barham, P. J.; Keller, A.; Otun, E. L. *J. Mater. Sci.* **1984**, *19*, 2781.
(5) Barham, P. J. J. *Mater. Sci.* **1984**, *19*, 3826.
(6) King, P. P. *J. Chem. Tech. Biotechnol.* **1982**, *32*, 2.
(7) Yasin, M.; Holland, S. J.; Jollly, A. M.; Tigbe, B. *J. Biomaterials* **1989**, *10*, 400.
(8) Scandola, M.; Ceccorulli, G.; Pizzoli, M. *Macromolecules*, **1992**, *25*, 6441.
(9) Marand, H.; Collins, M. *Polym. Prep. Am. Chem. Soc.* **1990**, *31*, 552.
(10) Azuma, Y.; Yoshie, N.; Sakurai, M.; Inoue, Y.; Chujo, R. *Polymer* **1992**, *33*, 4763.
(11) Avella, M.; Martuscelli, E. *Polymer* **1988**, *29*, 1731.
(12) Avella, M.; Greco, P.; Martuscelli, E. *Polymer* **1991**, *32*, 1647.
(13) Avela, M.; Martuscelli, E.; Raimo, M. *Polymer* **1993**, *34*, 3234.
(14) Greco, P.; Martuscelli, E. *Polymer* **1989**, *30*, 1475.
(15) Lotti, N.; Pizzoli, M.; Ceccorulli, G.; Scandola, M. *Polymer* **1993**, *34*, 35.
(16) Canetti, M.; Sadocco, P.; Siciliano, A.; Seves, A. *Polymer* **1994**, *35*, 2884.
(17) Paglia, E. D.; Beltrame, P. L.; Canetti, M.; Seves, A.; Marcandalli, B.; Martuscelli, E. *Polymer* **1993**, *34*, 996.
(18) Sadocco, P.; Canetti, M.; Seves, A.; Martuscelli, E. *Polymer* **1993**, *34*, 3368.
(19) Pearce, R.; Jesucason, J.; Orts, W.; Marchessault, R. H.; Bloembergen, S. *Polymer* **1992**, *33*, 4647.
(20) Pearce, R.; Brown, G. R.; Marchessault, R. H. *Polymer* **1994**, *35*, 3984.
(21) Pearce, R.; Marchessault, R. H. *Polymer* **1994**, *35*, 3990.
(22) Abe, H.; Doi, Y.; Satkowski, M. M.; Noda, I. *Macromolecules* **1994**, *27*, 50.
(23) Barker, P. A.; Mason, F.; Barham, P. J. *J. Mater. Sci.* **1990**, *25*, 1952.
(24) Organ, S. J. *Polymer* **1994**, *35*, 86.
(25) Iriondo, P.; Iruin, J. J.; Fernandez-Berridi, M. J. *Polymer* **1995**, *36*, 3235.
(26) Pomposo, J. A.; Cortazar, M.; Calahorra, E. *Macromolecules* **1994**, *27*, 245.
(27) Fox, T. G. *Bull. Am. Phys. Soc.* **1956**, 1, 123.
(28) Gordon, M.; Taylor, J. S. *J. Appl. Chem.* **1952**, *2*, 493.
(29) Couchman, P. R.; Karasz, F. E. *Macromolecules* **1978**, *11*, 117.
(30) Kwei, T. K. *J. Polym. Sci., Polym. Lett. Ed.* **1984**, *22*, 307.
(31) Pomposo, J. A.; Eguiazabal, I.; Calahorra, E.; Cortazar, M. *Polymer* **1993**, *34*, 95.
(32) Nishi, T.; Wang, T. T. *Macromolecules* **1975**, *8*, 915.
(33) Flory, P. J. *Principles of Polymer Chemistry*; Cornell University Press: Ithaca, NY, 1953.
(34) Hoffman, J. D.; Weeks, J. J. *J. Res. Natl. Bur. Stand.* **1962**, *66*, 13.
(35) Qin, C.; Pires, A. T. N.; Belfiore, L. A. *Polym. Commun.* **1990**, *31*, 177.
(36) Imken, R. L.; Paul, D. R.; Barlow, J. W. *Polym. Eng. Sci.* **1976**, *16*, 593.
(37) Paul, D. R.; Barlow, J. W.; Bernstein, R. E.; Wahrmund, D. S. *Polym. Eng. Sci.* **1978**, *18*, 1225.
(38) Ziska, J. J.; Barlow, J. W.; Paul, D. R. *Polymer*, **1981**, *22*, 918.
(39) Hoffman, J. D.; Davis, G. T.; Lauritzen, J. I., Jr. In *Treatise on Solid State Chemistry* Hannay, N. B., ED.; Plenum Press: New York, 1976; Vol. 3, Chapter 7.
(40) Hoffman, J. D. *Polymer* **1983**, *24*, 3.
(41) Williams, M. L.; Landel, R. F.; Ferry, J. D. *J. Am. Chem. Soc.* **1955**, *77*, 3701.
(42) Lauritzen, J.; Hoffman, J. D. *J. Appl. Phys.* **1973**, *44*, 4340.
(43) Roitman, D. B.; Marand, H.; Miller, R. L.; Hoffman, J. D. *J. Phys. Chem.* **1989**, *93*, 6929.
(44) Lovinger, A. J.; Davis, D. D.; Padden, F. J. *Polymer* **1985**, *26*, 1595.
(45) Keith, H. D.; Padden, F. J., Jr. *Polymer* **1984**, *25*, 28.
(46) Li, W.; Yan, R.; Jiang, B. *Polymer* **1992**, *33*, 889.
(47) Keith, H. D.; Padden, F. J. Jr. Results to be published.
(48) Defieuw, G.; Groeninckx, G.; Reynaers, H. *Polym. Commun.* **1989**, *30*, 267.
(49) Oudhuis, A. A. C. M.; Thiewes, H. J.; van Hutten, P. F.; ten Brinke, G. *Polymer* **1994**, *35*, 3936.

MA960615+